MicroRNA-466 inhibits osteosarcoma cell proliferation and induces apoptosis by targeting CCND1

WEI CAO[1], LE FANG[2], SIYONG TENG[3], HONGWEI CHEN[4] and TIEJUN LIU[5]

[1]Clinical Laboratory, Beijing Rehabilitation Hospital of Capital Medical University, Beijing 100041;
[2]Department of Blood Transfusion, 521 Hospital of Ordnance Industry, Xi'an, Shaanxi 710065;
[3]Department of Cardiovascular Medicine, National Center for Cardiovascular Diseases, Beijing 102300;
[4]Clinical Laboratory, Shanghai Songjiang District Central Hospital, Shanghai 201600;
[5]Department of Urology, Beijing Rehabilitation Hospital of Capital Medical University, Beijing 100144, P.R. China

Received April 28, 2018; Accepted August 30, 2018

DOI: 10.3892/etm.2018.6888

Abstract. Emerging pieces of evidence indicate that microRNA-466 (miR-466) serves as a tumor suppressor in several human tumors, including colorectal cancer and prostate cancer. However, whether miR-466 is involved in osteosarcoma (OS) progression remains largely unknown. The present study demonstrated that miR-466 was significantly downregulated in OS tissues and cell lines. Furthermore, it was revealed that the expression of miR-466 was negatively correlated with OS severity. Moreover, low miR-466 expression in patients with OS predicted poor prognosis. Through functional experiments, miR-466 overexpression significantly inhibited the proliferation and cell cycle of OS cells while inducing cellular apoptosis. In terms of mechanism, it was revealed that CCND1 was a target of miR-466 in OS cells. miR-466 overexpression suppressed CCND1 expression in OS cells. A reverse association was observed between the expression levels of miR-466 and CCND1 in OS tissues. Furthermore, CCND1 restoration in OS cells significantly rescued the effects of miR-466 on cellular proliferation and apoptosis. Overall, the results of the present study demonstrated that miR-466 suppressed OS progression by targeting CCND1, suggesting that miR-466 may be a promising biomarker and therapeutic target for OS prognosis and treatment.

Introduction

Osteosarcoma (OS) is one of the most prevalent and aggressive bone tumors and leads to high mortality rates in children and adolescents (1). OS accounts for approximately 66% cases of bone cancers worldwide (2). Although great effort has been made in the past decades, advance achievement on OS treatment remains very limited, and the outcomes of patients with OS are quite poor (3). Nowadays, surgical resection combined with chemotherapy and radiotherapy is the main approach for OS treatment. However, this method has a poor effect on advanced or metastatic OS (4). Therefore, searching novel biomarkers for early diagnosis of patients with OS and effective targets for OS therapy is urgently required.

MicroRNAs (miRNAs) are a class of short noncoding RNAs of approximately 22-25 nucleotides in length and has been demonstrated to regulate gene expression by binding to the three prime untranslated region (3'-UTR) of target mRNAs for degradation (5). In the past decades, large numbers of studies showed that miRNAs exert very important functions in almost all kinds of biological processes, such as cell survival, proliferation, migration, and invasion (6-8). Especially in cancer, the miRNA functions have been widely explored. For example, Du *et al* (9), reported that microRNA-509-3p represses glioma cell proliferation and invasion. Wang *et al* (10), showed that microRNA-124-3p suppresses the growth and metastasis of cervical cancer. In OS, several miRNAs have also been reported to exert essential functions, such as microRNA-643 (11), microRNA-138 (12), and microRNA-27a (13).

Two recent reports indicate that miR-466 inhibits tumor growth and metastasis in prostate cancer and colorectal cancer (14,15). Nevertheless, the function of miR-466 in OS remains elusive. In the present study, we found that miR-466 was significantly downregulated in OS tissues. The expression level of miR-466 was negatively associated with OS severity. Through functional experiments, we demonstrated that miR-466 suppressed OS cell proliferation and induced cellular apoptosis. Mechanistically, we found that CCND1 was a target of miR-466 in OS cells. CCND1 restoration abrogated the effects of miR-466 transfection in OS cells. In a word, our study demonstrated that miR-466 served as a tumor suppressor through targeting CCND1 and implied that miR-466 might be a promising prognostic biomarker and therapeutic target.

Materials and methods

Cell lines and clinical specimens. The OS cell lines used in the present study, including 143B, U2OS, KHOS-240S, Saos-2 and

Correspondence to: Professor Tiejun Liu, Department of Urology, Beijing Rehabilitation Hospital of Capital Medical University, Xixia Zhuang, Badachu Road, Shijingshan, Beijing 100144, P.R. China
E-mail: liutiejun612@163.com

Key words: miR-466, CCND1, proliferation, apoptosis, osteosarcoma

MG-63, and the normal cell line (hFOB1.19) were purchased from The Shanghai Institute of Cell Biology (Shanghai, China). The cells were maintained in RPMI-1640 medium supplemented by 10% fetal bovine serum (FBS), streptomycin (100 μg/ml) and penicillin (200 U/ml; all from Sigma-Aldrich; Merck KGaA, Darmstadt, Germany) in 5% CO_2 at 37˚C. A total of 87 surgically resected OS specimens and adjacent normal tissues were acquired from patients at Beijing Rehabilitation Hospital of Capital Medical University between June 2013 and August 2016. All patients signed formal consent forms. The experiments involving human specimens were reviewed and approved by the Ethics Committee of Beijing Rehabilitation Hospital of Capital Medical University.

Cell transfection. For CCND1 overexpression, the coding sequence of CCND1 was constructed into pCDNA3-myc vector (pCDNA3-myc-CCND1). The miR-466 mimics, miR-466 inhibitor and negative controls were synthesized and purchased from Sigma-Aldrich; Merck KGaA. Corresponding plasmids were transfected into 143B and U2OS cells using Lipofectamine® 2000 (Invitrogen; Thermo Fisher Scientific, Inc., Waltham, MA, USA), according to the manufacturer's protocol. After incubation for 48 h, cells were used for further analysis.

Cell proliferation assay. For cell proliferation assays, the viable cells were tested by Cell Counting Kit-8 (CCK-8) assay kit according to the manufacturer's instructions. In brief, cells were grown in 96-well plate with $1x10^4$ per well and incubated in 37˚C with 5% CO_2 until cell confluent rate reached 70%. After transfected with plasmid for 48 h, cells were still incubated for 24, 48, 72 and 96 h. 10 μl CCK8 solution was seed into each well. The absorbance at 490 nm was measured with SUNRISE Microplate Reader (Tecan Group, Ltd., Mannedorf, Switzerland).

Reverse transcription-quantitative polymerase chain reaction (RT-qPCR). Total RNA was extracted from tissues and cells using the RNeasy Plus mini kit (Qiagen GmbH, Hilden, Germany), according to the manufacturer's instructions. RNA was then reversely transcribed into complementary DNA using the PrimeScript RT-PCR kit (Takara Biotechnology Co., Ltd., Dalian, China) according to the manufacturer's instructions. For quantification, PCR was performed using a miRNA Q-PCR Detection kit (GeneCopoeia, Inc., Rockville, MD, USA) on an ABI 7500 thermocycler (Thermo Fisher Scientific, Inc.). U6 or GAPDH was used as an internal reference. The relative expression of mRNA was determined using the $2^{-\Delta\Delta Cq}$ method (16). The primer sequences were as follows: miR-466 (5'-AACGAGACGACGACAGAC-3' and 5'-ATACACATA CACGCAACACACAT-3'), U6 (5'-AACGAGACGACGACA GAC-3' and 5'-GCAAATTCGTGAAGCGTTCCATA-3'), CCND1 (5'-TGAGGGACGCTTTGTCTGTC-3' and 5'-GCC TTTGGCCTCTCGATACA-3') and GAPDH (5'-ATGTTG CAACCGGGAAGGAA-3' and 5'-AGGAAAAGCATCACC CGGAG-3').

Western blot analysis. Total proteins were isolated by radioimmunoprecipitation (RIPA) assay buffer (Wlaterson, Barcelona, Spain). Protein concentration was determined using a bicinchoninic acid (BCA) protein assay kit (Wlaterson). A total of 50 μg protein was separated by 12% sodium dodecyl sulfate polyacrylamide gels (SDS-PAGE), and transferred to polyvinylidene fluoride (PVDF) membranes (EMD Millipore, Billerica, MA, USA). The membranes were blocked with 10% skim milk (w/v) at room temperature for 2 h. Target proteins were probed with specific antibodies against Cyclin D1 (1:2,000; cat. no. 2978; Cell Signaling Technology, Inc., Danvers, MA, USA) and GAPDH (1:5,000; cat. no. 5174; Cell Signaling Technology, Inc.), followed by incubation with horseradish peroxidase conjugated goat-anti-rabbit second antibody (1:5,000; cat. no. 7074; Cell Signaling Technology Inc.). The blots were detected with the Enhanced Chemiluminescence western blot detection kit (Pierce; Thermo Fisher Scientific, Inc.).

Statistical analysis. Each experiment was repeated at least three times. All data are expressed in terms of means ± SD. The Kaplan-Meier method was used to calculate the survival curve, and log-rank test to determine statistical significance. The differences between groups were analyzed using Two-tail Student's t-test and ANOVA followed by Tukey's post hoc test. Pearson correlation coefficient analysis was used to determine the expression correlation between CCND1 and miR-466. Chi-square test was used for analysis of correlation between miR-466 expression and clinicopathological characteristics. $P<0.05$ was considered to indicate a statistically significant difference.

Results

MiR-466 is downregulated in OS tissues. To explore the function of miR-466, we determined its expression in OS tissues and adjacent normal tissues by RT-qPCR. The results indicated that miR-466 was significantly downregulated in OS tissues (n=87) compared with adjacent normal tissues (n=87; Fig. 1A). Consistently, miR-466 expression was also downregulated in OS cell lines, including 143B, U2OS, KHOS-240S, UMR-106, Saos-2, and MG-63 cells compared with hFOB1.19 cells (Fig. 1B). Then, we divided these OS samples into two groups based on miR-466 expression level and analyzed the correlation between miR-466 expression and clinicopathological characteristics. We found that miR-466 expression in OS tissues was negatively correlated with differentiation, tumor metastasis, and tumor, node, and metastasis (TNM) stage, whereas no significant correlation was observed with age and gender (Table I). Furthermore, we performed Kaplan-Meier curve to determine the relationship between miR-466 expression and prognosis of patients with OS. The results showed that high expression of miR-466 in patients with OS was linked to high survival rate (Fig. 1C). Overall, our data indicated that miR-466 was downregulated in OS tissues and correlated with patients' severity and prognosis, implying that miR-466 may exert an important role in OS progression.

MiR-466 suppresses OS cell proliferation and induces apoptosis. To investigate the physiological functions of miR-466, we selected 143B and U2OS cells for the following experiments. We effectively knocked down or overexpressed miR-466 in 143B and U2OS cells by transfection with miR-466 mimic or inhibitor (Fig. 2A). Then, we performed CCK8 assays to

Table I. Correlation between miR-466 expression and clinicopathological characteristics in OS tissues.

Variables	n=87	Low (n=44)	High (n=43)	P-value
Age, years				0.605
<60	68	33	35	
≥60	19	11	8	
Sex				0.670
Male	45	24	21	
Female	42	20	22	
Differentiation				0.001
Well/moderate	45	15	30	
Poor	42	29	13	
Metastasis				0.003
Absent	42	14	28	
Present	45	30	15	
TNM stage				0.018
I-II	45	17	28	
III-IV	42	27	15	

TNM, tumor node metastasis.

measure cell proliferation. We found that miR-466 overexpression significantly inhibited the proliferation of 143B and U2OS cells, and vice versa (Fig. 2B and C). To explore whether the reduced cell proliferation is induced by aberrant cell cycle, we stained 143B and U2OS cells with PI and performed FACS analysis. The results indicated that miR-466 overexpression significantly increased the percent of cells in G0/G1 phase and decreased cells in S phase, and vice versa (Fig. 2D and E). Furthermore, we found that miR-466 overexpression remarkably promoted the percentages of apoptotic 143B and U2OS cells (Fig. 2F). Collectively, these results indicated that miR-466 suppressed OS cell proliferation and induced apoptosis.

CCND1 is a target of miR-466. Then, we investigated the molecular mechanism of miR-466. Through bioinformatics analysis, we found that CCND1 encoding Cyclin D1 was a potential target of miR-466. A potential binding site of miR-466 in the 3'-UTR region of CCND1 mRNA was observed (Fig. 3A). Then, we constructed CCND1-3'-UTR-WT or mutant (MUT) luciferase reporter plasmid for luciferase reporter assays. The results demonstrated that miR-466 overexpression significantly inhibited the luciferase activity in 143B and U2OS cells transfected with CCND1-3'-UTR-WT (Fig. 3B and C). However, mutation of the potential binding site in the 3'-UTR region of CCND1 mRNA abrogated the effect of miR-466 transfection (Fig. 3B and C). Moreover, RT-qPCR and Western blot results showed that miR-466 overexpression inhibited the mRNA and protein levels of CCND1 in 143B and U2OS cells (Fig. 3D and E). We also found that the miR-466 expression was reversely correlated with that of CCND1 in OS tissues (Fig. 3F). Moreover, we found that CCND1 was also highly expressed in OS tissues compared with adjacent normal tissues (Fig. 3G). Overall, above results demonstrated that CCND1 is a direct target of miR-466 in OS cells.

Overexpression of CCND1 counteracts the effects of miR-466 transfection in OS cells. To further validate that CCND1 is important for the function of miR-466 in OS cells, we performed rescue experiments. We restored the protein levels of CCND1 in 143B and U2OS cells transfected with miR-466 mimics. We successfully overexpressed CCND1 in 143B and U2OS cells (Fig. 4A). And western blot results also indicated that CCND1 was significantly upregulated in 143B and U2OS cells (Fig. 4A). Obviously, miR-466 overexpression inhibited the proliferation and cell cycle, whereas CCND1 restoration enhanced cell proliferation and cell cycle in 143B and U2OS cells (Fig. 4B-E). Consistently, miR-466 overexpression promoted cell apoptosis, whereas CCND1 overexpression reduced apoptotic cells (Fig. 4F). These results further confirmed that miR-466 exerted tumor-suppressive function through targeting CCND1.

Discussion

OS is the most prevalent and malignant bona fide tumor in adolescents and children and has become a serious threat for human life. No effective therapeutic method for OS complete healing is available to date. The molecular pathogenesis of OS still remains elusive. MiRNAs are a type of short noncoding RNAs and have been reported to regulate gene expression post-transcriptionally. In the past decades, accumulating studies demonstrate the essential roles of miRNAs in human cancers through regulating all aspects of bioactivities, such as development, proliferation, metabolism, and invasion (17,18). In addition, several pieces of evidence have demonstrated a close relationship between miRNA and OS progression (19,20). Therefore, understanding the underlying mechanism of miRNA in OS development and progression may provide a novel orientation for diagnosis, prognosis, and therapy of patients with OS. In the present study, we identified miR-446 as a tumor suppressor in OS.

Previous reports showed that miR-446 acts as a tumor suppressor in several cancers, such as prostate cancer and colorectal cancer (14,15). Besides, Sun *et al* (21), reported that the expression levels of miR-466 were higher in cervical cancer tissues than that in adjacent normal controls. However, whether miR-466 plays a function in OS needs to be investigated. In this study, we found that miR-466 was also significantly downregulated in OS tissues and cell lines compared with adjacent normal control. Furthermore, we found that miR-466 expression levels were negatively correlated with tumor TNM stage and metastasis. Additionally, we showed that miR-466 downregulation predicted a poor prognosis in patients with OS. Through functional experiments, we found that miR-466 overexpression significantly inhibited the proliferation and induced cellular apoptosis in OS cells. These data suggested that miR-466 also served as a tumor suppressor in OS. However, although we found a correlation between miR-466 expression and metastasis, whether miR-466 regulates OS cell metastasis requires to be further investigated by functional experiments.

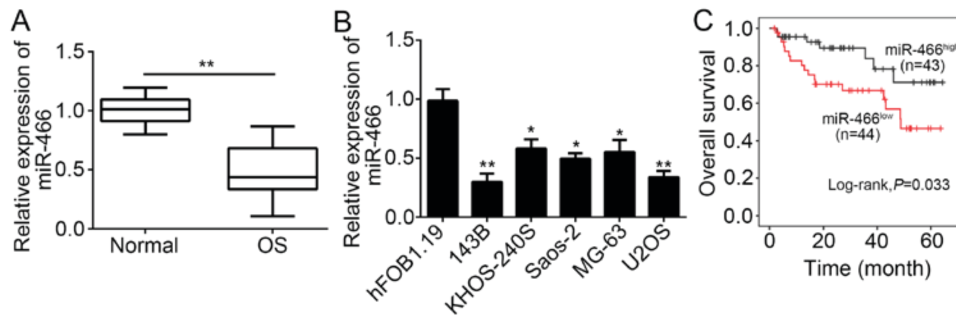

Figure 1. MiR-466 is downregulated in OS tissues. (A) Relative expression of miR-466 in 87 pairs of OS tissues and adjacent normal tissues by RT-qPCR analysis. (B) Expression patterns of miR-466 in OS cell lines by RT-qPCR. (C) Kaplan-Meier analysis was used to determine the probabilities of overall survival in patients with OS according to miR-466 expression. *P<0.05 and **P<0.01 vs. control group. OS, osteosarcoma.

Figure 2. MiR-466 suppresses OS cell proliferation and induces apoptosis. (A) Relative expression levels of miR-466 in 143B and U2OS cells transfected with miR-466 mimic, inhibitor or negative control (NC) by RT-qPCR. CCK8 assays were used to determine the proliferation of (B) 143B and (C) U2OS cells. Cell cycle distribution was determined by FCAS in (D) 143B and (E) U2OS cells stained with PI. (F) Cellular apoptosis was measured by FACS in 143B and U2OS cells stained with Annexin V/PI. *P<0.05 and **P<0.01 vs. control group. OS, osteosarcoma.

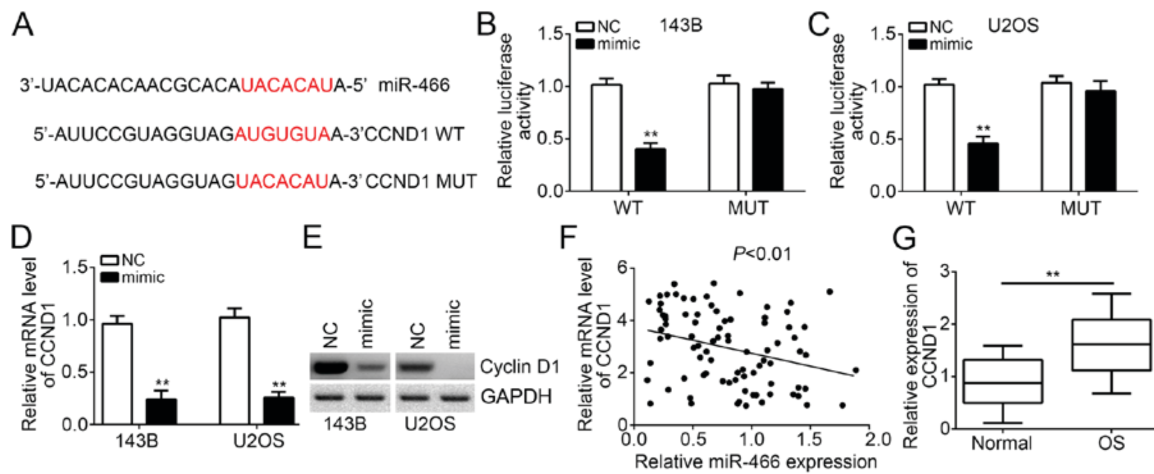

Figure 3. CCND1 s a target of miR-466. (A) Predicted binding site of miR-466 in the 3'-UTR region of CCND1 mRNA. Luciferase reporter assays indicated that miR-466 overexpression inhibited the luciferase activity in (B) 143B and (C) U2OS cells transfected with WT-CCND1-3'-UTR. (D) RT-qPCR analysis indicated that miR-466 overexpression suppressed the mRNA levels of CCND1. (E) Western blot analysis showed that miR-466 overexpression inhibited the protein level of Cyclin D1 in 143B and U2OS cells. GAPDH was used as the loading control. (F) Correlation between the levels of miR-466 and CCND1 in OS tissues was determined by RT-qPCR. (G) Relative expression of CCND1 in OS tissues and normal tissues by RT-qPCR. **P<0.01 vs. control group.

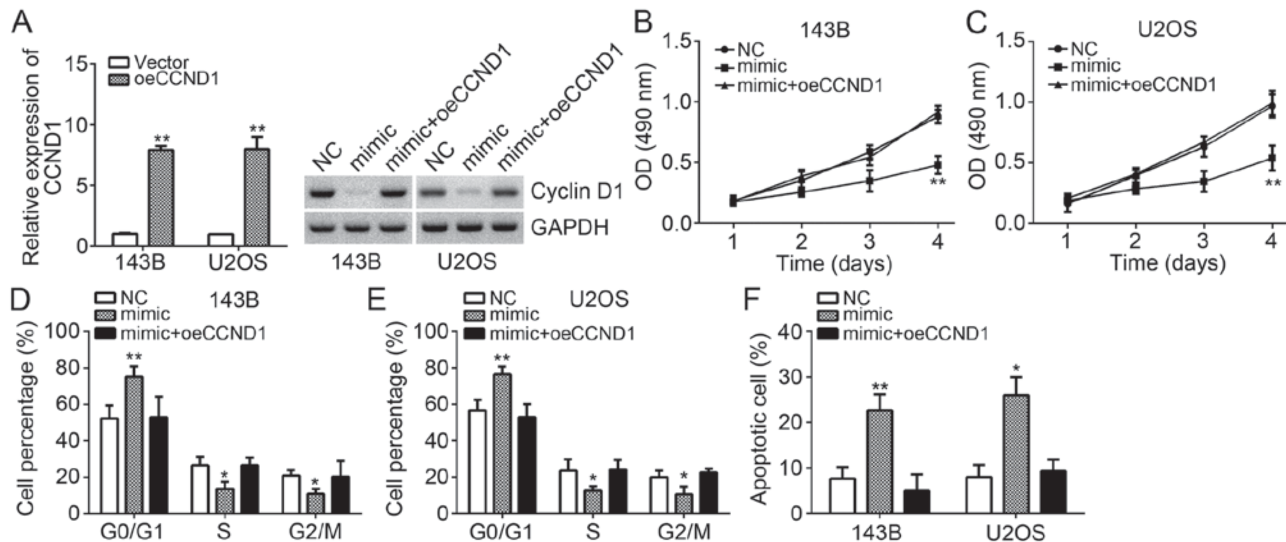

Figure 4. CCND1 overexpression counteracts the effects of miR-466 transfection in OS cells. (A) The mRNA and protein levels of CCND1 were measured by RT-qPCR and western blot in 143B and U2OS cells. CCK8 assays were used to determine the proliferation of (B) 143B and (C) U2OS cells. Cell cycle distribution in (D) 143B and (E) U2OS cells were analyzed by FACS. (F) Cellular apoptosis was measured by FACS in 143B and U2OS cells stained with Annexin V/PI. *P<0.05 and **P<0.01 vs. control group. OS, osteosarcoma.

CCND1 encoding Cyclin D1 is a member of cyclin family and plays a key role in regulating cell cycle progression (22). Increasing evidence indicated that CCND1 exerts an essential role in promoting the development and progression of human cancers, such as gastric cancer (23), glioma (24), renal cell cancer (25), lung adenocarcinoma (26) and (27). Except regulation of cell cycle, recent reports also indicated that CCND1 has a pivot role in promoting migration and tumor metastasis (28). Another study showed that Cyclin D1 recruits HDACs or histone methyltransferases to regulate gene transcription (29). To explore the mechanism of CCND1 expression is important because of the extensive roles of CCND1 in cancer. In our study, we identified CCND1 as a direct target of miR-446. We showed that miR-446 overexpression significantly inhibited the CCND1 expression in 143B and U2OS cells. Moreover, a reverse correlation was observed between their expression levels in OS tissues. Through functional experiments, we demonstrated that CCND1 restoration markedly rescued the effects of miR-446 overexpression on OS cell proliferation and apoptosis.

In conclusion, our results showed that miR-446 is significantly downregulated and inversely correlated with CCND1 expression in OS tissues. Besides, these data demonstrated that miR-446 serves as a tumor suppressor and might be a promising biomarker for prognosis of patients with OS. This study also implied that miR-446 might serve as a potential therapeutic target for OS treatment.

Acknowledgements

Not applicable.

Funding

No funding was received.

Availability of data and materials

All data generated or analyzed during the present study are included in this published article.

Authors' contributions

WC and TL initiated and designed the present study, analyzed and interpreted the results, and wrote this manuscript. LF, ST and HC performed certain experiments. All authors read and approved the final manuscript.

Ethics approval and consent to participate

For the use of human samples, the protocol for this study was approved by the Institutional Ethics Committee of Hospital of Capital Medical University and all enrolled patients signed a written informed consent document.

Patient consent for publication

All patients within the present study provide consent for the publication of their data.

Competing interests

The authors declare that they have no competing interests.

References

1. Heare T, Hensley MA and Dell'Orfano S: Bone tumors: Osteosarcoma and Ewing's sarcoma. Curr Opin Pediatr 21: 365-372, 2009.
2. Shackleton M, Quintana E, Fearon ER and Morrison SJ: Heterogeneity in cancer: Cancer stem cells versus clonal evolution. Cell 138: 822-829, 2009.
3. Levings PP, McGarry SV, Currie TP, Nickerson DM, McClellan S, Ghivizzani SC, Steindler DA and Gibbs CP: Expression of an exogenous human Oct-4 promoter identifies tumor-initiating cells in osteosarcoma. Cancer Res 69: 5648-5655, 2009.
4. Fagioli F, Aglietta M, Tienghi A, Ferrari S, Brach del Prever A, Vassallo E, Palmero A, Biasin E, Bacci G, Picci P and Madon E: High-dose chemotherapy in the treatment of relapsed osteosarcoma: An Italian sarcoma group study. J Clin Oncol 20: 2150-2156, 2002.
5. Ambros V: The functions of animal microRNAs. Nature 431: 350-355, 2004.
6. Yang Y, Jiang Z, Ma N, Wang B, Liu J, Zhang L and Gu L: MicroRNA-223 targeting STIM1 inhibits the biological behavior of breast cancer. Cell Physiol Biochem 45: 856-866, 2018.
7. Zavala-Yoe R, Ramirez-Mendoza RA and Cordero LM: Entropy measures to study and model long term simultaneous evolution of children in Doose and Lennox-Gastaut syndromes. J Integr Neurosci 15: 205-221, 2016.
8. Cui Y, Chen LG, Yao HB, Zhang J and Ding KF: Upregulation of microRNA-383 inhibits the proliferation, migration and invasion of colon cancer cells. Oncol Lett 15: 1184-1190, 2018.
9. Du P, Luan X, Liao Y, Mu Y, Yuan Y, Xu J and Zhang J: MicroRNA-509-3p inhibits cell proliferation and invasion via downregulation of X-linked inhibitor of apoptosis in glioma. Oncol Lett 15: 1307-1312, 2018.
10. Wang P, Zhang L, Zhang J and Xu G: MicroRNA-124-3p inhibits cell growth and metastasis in cervical cancer by targeting IGF2BP1. Exp Ther Med 15: 1385-1393, 2018.
11. Wang H, Xing D, Ren D, Feng W, Chen Y, Zhao Z, Xiao Z and Peng Z: MicroRNA-643 regulates the expression of ZEB1 and inhibits tumorigenesis in osteosarcoma. Mol Med Rep 16: 5157-5164, 2017.
12. Zhou Z, Li Z, Shen Y and Chen T: MicroRNA-138 directly targets TNFAIP8 and acts as a tumor suppressor in osteosarcoma. Exp Ther Med 14: 3665-3673, 2017.
13. Lin T, Ma Q, Zhang Y, Zhang H, Yan J and Gao C: MicroRNA-27a functions as an oncogene in human osteosarcoma by targeting CCNG1. Oncol Lett 15: 1067-1071, 2018.
14. Colden M, Dar AA, Saini S, Dahiya PV, Shahryari V, Yamamura S, Tanaka Y, Stein G, Dahiya R and Majid S: MicroRNA-466 inhibits tumor growth and bone metastasis in prostate cancer by direct regulation of osteogenic transcription factor RUNX2. Cell Death Dis 8: e2572, 2017.
15. Tong F, Ying Y, Pan H, Zhao W, Li H and Zhan X: MicroRNA-466 (miR-466) functions as a tumor suppressor and prognostic factor in colorectal cancer (CRC). Bosn J Basic Med Sci, Jan 17, 2018 (Epub ahead of print).
16. Livak KJ and Schmittgen TD: Analysis of relative gene expression data using real-time quantitative PCR and the 2(-Delta Delta C(T)) method. Methods 25: 402-408, 2001.
17. Huang Y, Shen XJ, Zou Q, Wang SP, Tang SM and Zhang GZ: Biological functions of microRNAs: A review. J Physiol Biochem 67: 129-139, 2011.
18. Wang ZM, Wan XH, Sang GY, Zhao JD, Zhu QY and Wang DM: miR-15a-5p suppresses endometrial cancer cell growth via Wnt/β-catenin signaling pathway by inhibiting WNT3A. Eur Rev Med Pharmacol Sci 21: 4810-4818, 2017.
19. Nugent M: microRNA and bone cancer. Adv Exp Med Biol 889: 201-230, 2015.
20. Gao X, Han D and Fan W: Down-regulation of RBP-J mediated by microRNA-133a suppresses dendritic cells and functions as a potential tumor suppressor in osteosarcoma. Exp Cell Res 349: 264-272, 2016.
21. Sun P, Shen Y, Gong JM, Zhou LL, Sheng JH and Duan FJ: A new MicroRNA expression signature for cervical cancer. Int J Gynecol Cancer 27: 339-343, 2017.
22. Zhao M, Xu P, Liu Z, Zhen Y, Chen Y, Liu Y, Fu Q, Deng X, Liang Z, Li Y, *et al*: Dual roles of miR-374a by modulated c-Jun respectively targets CCND1-inducing PI3K/AKT signal and PTEN-suppressing Wnt/β-catenin signaling in non-small-cell lung cancer. Cell Death Dis 9: 78, 2018.
23. Huang H, Han Y, Yang X, Li M, Zhu R, Hu J, Zhang X, Wei R, Li K and Gao R: HNRNPK inhibits gastric cancer cell proliferation through p53/p21/CCND1 pathway. Oncotarget 8: 103364-103374, 2017.
24. Chen DG, Zhu B, Lv SQ, Zhu H, Tang J, Huang C, Li Q, Zhou P, Wang DL and Li GH: Inhibition of EGR1 inhibits glioma proliferation by targeting CCND1 promoter. J Exp Clin Cancer Res 36: 186, 2017.
25. Xue J, Qin Z, Li X, Zhang J, Zheng Y, Xu W, Cao Q and Wang Z: Genetic polymorphisms in cyclin D1 are associated with risk of renal cell cancer in the Chinese population. Oncotarget 8: 80889-80899, 2017.
26. Yao Y, Luo J, Sun Q, Xu T, Sun S, Chen M, Lin X, Qian Q, Zhang Y, Cao L, *et al*: HOXC13 promotes proliferation of lung adenocarcinoma via modulation of CCND1 and CCNE1. Am J Cancer Res 7: 1820-1834, 2017.
27. Wu J, Cui LL, Yuan J, Wang Y and Song S: Clinical significance of the phosphorylation of MAPK and protein expression of cyclin D1 in human osteosarcoma tissues. Mol Med Rep 15: 2303-2307, 2017.
28. Li Z, Wang C, Prendergast GC and Pestell RG: Cyclin D1 functions in cell migration. Cell Cycle 5: 2440-2442, 2006.
29. Fu M, Rao M, Bouras T, Wang C, Wu K, Zhang X, Li Z, Yao TP and Pestell RG: Cyclin D1 inhibits peroxisome proliferator-activated receptor gamma-mediated adipogenesis through histone deacetylase recruitment. J Biol Chem 280: 16934-16941, 2005.

This work is licensed under a Creative Commons Attribution-NonCommercial-NoDerivatives 4.0 International (CC BY-NC-ND 4.0) License.